The effect of relative humidity and temperature on the response of stomatal conductance to vapor pressure deficit in tropical trees

Julien Lamour[1], Kenneth J. Davidson[2], Jérôme Chave[1], Martijn Slot[3], Shawn P. Serbin[4], Alistair Rogers[5]

[1]Centre de Recherche sur la Biodiversité et l'Environnement (CRBE), Université de Toulouse, CNRS, IRD, Toulouse INP, Université Toulouse 3 – Paul Sabatier (UT3), Toulouse, France

[2]American Forests, Washington, DC 20005, USA

[3]Smithsonian Tropical Research Institute, Balboa, Ancon, Republic of Panama

[4]Biospheric Sciences Laboratory (BSL), Code 618 NASA Goddard Space Flight Center 8800 Greenbelt Road Greenbelt, MD 20771 USA

[5]Climate and Ecosystems Sciences Division, Lawrence Berkeley National Laboratory, Berkeley CA 94720, USA

Corresponding author: Julien Lamour: jlamour.sci@gmail.com

Introduction	M and M	Results	Discussion	Conclusions	Total
998	2252	1283	1914	226	6673

Tables: 3, Figures: 6

Supplementary Tables: 5, Supplementary Figures: 7

Name	Orcid	Email
Julien Lamour	0000-0002-4410-507X	jlamour.sci@gmail.com
Kenneth J. Davidson	0000-0001-5745-9689	kdavidson@americanforests.org
Jérôme Chave	0000-0002-7766-1347	jerome.chave@univ-tlse3.fr
Martijn Slot	0000-0002-5558-1792	SlotM@si.edu
Shawn P. Serbin	0000-0003-4136-8971	shawn.p.serbin@nasa.gov
Alistair Rogers	0000-0001-9262-7430	alistair@lbl.gov

Short title (50 characters, space included): The stomatal response to VPD in tropical trees

Highlight

Gas exchange measurements in five tropical trees show a nonlinear coupling between photosynthesis and stomatal conductance when relative humidity and temperature vary. Stomatal models fail at representing the conductance response to high relative humidity.

Abstract

Understanding how leaf gas exchange responds to changes in vapor pressure deficit (VPD) is key to predicting tropical forest resilience to climate change. Stomata regulate leaf water and CO_2 diffusion, and respond to changes in temperature and relative humidity, two drivers of VPD. At high temperatures, the cuticular pathway may also become significant and participate in the overall leaf conductance. Here, we measured gas exchange under light and dark conditions to investigate the stomatal and cuticular responses to temperature and relative humidity on detached branches in five tropical tree species. Leaf conductance in the dark, when stomata are essentially closed, was not markedly impacted by temperature and relative humidity, suggesting a minimal response of the cuticular pathway to these conditions. We compared six steady-state conductance models incorporating different effects of photosynthesis and evaporative demand on stomatal control. All models performed well (RMSE < 0.025 mol m^{-2} s^{-1}), but the best-fitting model (RMSE = 0.017 mol m^{-2} s^{-1}) used a nonlinear relationship between photosynthesis and stomatal conductance and incorporated relative humidity rather than vapor pressure difference. All models overestimated the steady-state conductance at high relative humidity. Furthermore, leaf conductance immediately increased after a decrease in relative humidity (wrong-way response), but not after an increase in leaf temperature. This suggests that the mechanisms underlying stomatal response to VPD need further investigation. The non-linear coupling between photosynthetic rate and stomatal conductance indicates a sharper physiological response than previously acknowledged.

Introduction

Tropical forests are critical global carbon sinks, but their future productivity and their role as an important global carbon store are uncertain in a changing environment. Increased atmospheric CO_2 concentration stimulates photosynthesis and increases plant growth (Ainsworth & Rogers, 2007; Reich & Hobbie, 2013), whereas higher temperatures and higher vapor pressure deficit

(VPD) may have the opposite effect, limiting carbon acquisition and increasing tree mortality (Way *et al.*, 2015; McDowell *et al.*, 2018; Grossiord *et al.*, 2020).

Stomata lie at the nexus of these processes. They cover only a small fraction of the leaf surface but constitute the main pathway for gas exchange. They provide dynamic control of transpiration and respond to increasing CO_2 concentration, temperature, and VPD, as well as decreasing soil moisture content (Zhou *et al.*, 2013). Whether climate change will increase or decrease tropical forest growth thus largely depends on how stomata respond to environmental conditions (Lloyd & Farquhar, 2008; Franks *et al.*, 2013; Brodribb *et al.*, 2020).

Of particular importance is the role of projected higher temperature and VPD on the stomatal conductance of tropical tree species (McDowell *et al.*, 2018; Doughty *et al.*, 2023). 85% of atmospheric water vapor originates from evaporation from the ocean surface, far ahead of continental evapotranspiration (Trenberth et al., 2007). Projections that account for a changing climate indicate that the temperature difference between oceans and continents is expected to increase. Rising ocean surface temperatures increase the specific humidity of air masses transported over continents, but the greater increase in continental temperature effectively reduces the relative humidity of the air and increases VPD (Byrne & O'Gorman, 2016), which is the main driver of plant transpiration. The increase in VPD observed in many tropical forest basins (Fang *et al.*, 2022; Mu *et al.*, 2025) is a factor that already limits the positive effect of rising CO_2 on vegetation growth (Yuan *et al.*, 2019). Stomatal closure, driven by the decrease in VPD and the increase in temperature, may further reduce transpiration and air moisture recycling and amplify the negative effect on forest growth (Brando *et al.*, 2025). Improved understanding and model representation of the stomatal response to high temperature and VPD is therefore critical to improve understanding and model representation of tropical forests.

In Earth System Models, steady-state leaf conductance (g_{sw}) is commonly modeled by a linear relationship (Equation 1) where g_{sw} responds to the product of functions of photosynthesis *f(A)*, CO_2 concentration *f(CO_2)*, and evaporative demand *f(VPD)* (Damour *et al.*, 2010).

$$g_{sw} = g_0 + g_1 f(A) f(CO_2) f(VPD) \quad (1)$$

In this relationship, g_0 is a parameter representing the basal conductance primarily attributed to gas exchange through the cuticle and imperfectly closed stomata (Duursma *et al.*, 2019; Márquez *et al.*, 2021; Lamour *et al.*, 2022b). This parameter represents nonzero conductance in

the dark and is key in determining night transpiration, as well as species vulnerability to drought (Barnard & Bauerle, 2013; Choat *et al.*, 2018). The second parameter, $g_{1,}$ scales the sensitivity of g_{sw} to environmental drivers. It is inversely related to leaf water use efficiency and varies at multiple scales, including among individuals, species, biomes, and seasons (Lin *et al.*, 2015; Franks *et al.*, 2017; Wolz *et al.*, 2017).

The functions *f(A)*, *f(CO_2),* and *f(VPD)* have multiple versions stemming from early empirical models of stomatal conductance and more recent theories for modelling optimal stomatal behaviour (Damour *et al.*, 2010; Medlyn *et al.*, 2011). For instance, the effect of air vapor demand on g_{sw}, *f(VPD)*, has been modeled by a direct effect of the relative humidity (*RH*) at the leaf surface (Ball *et al.*, 1987) or by the response to the leaf-to-air vapor pressure difference (VPD_{leaf}) (Medlyn *et al.*, 2011). VPD_{leaf} is typically considered the most accurate variable as it is the driving force for the process of transpiration (Mott & Parkhurst, 1991; Monteith, 1995). However, uncertainty remains regarding the choice of the *f(VPD)* function because stomata respond indirectly to changes in transpiration rate (Buckley, 2019), and their response is complex and modulated by both hydraulic and chemical signals (Buckley, 2016; McAdam *et al.*, 2016). In addition, the proposal by Ball and Berry to use *f(VPD) = RH* to model the quantitative response of stomata was pragmatic since part of the effect of temperature on g_{sw} was taken into account through *f(A)* (Collatz *et al.*, 1991).

The dependence of stomatal conductance on the photosynthesis rate *f(A)* is commonly modeled by a linear relationship (Damour *et al.*, 2010). Several lines of evidence support a close relationship between photosynthesis and stomatal conductance, although the photosynthesis-related signal perceived by the stomata has yet to be discovered (Busch, 2014; Lawson & Matthews, 2020). However, evidence suggests a nonlinear relationship between *A* and g_{sw} when the light varies (Ball, 1988; Kromdijk *et al.*, 2019; Lamour *et al.*, 2022a). This nonlinearity is captured in models where stomata respond to a photosynthesis dependent signal (Buckley *et al.*, 2003; Busch, 2014; Kromdijk *et al.*, 2019) or in stomatal optimization models that account for a limitation of photosynthesis by electron transport rate at low light and carboxylation rate at high light (Lamour *et al.*, 2022a).

Other uncertainties in the g_{sw} response to *VPD* are associated with the role of the cuticular pathway represented through g_0. While g_0 is often considered constant in models, the physical properties of the cuticle may vary with temperature or *RH*, confounding the effect of these

variables on stomatal conductance. In particular, the increase in g_{sw} at high temperatures observed in some studies (Slot *et al.*, 2016; Urban *et al.*, 2017; Drake *et al.*, 2018) may be due to an increase in cuticular conductance (Cochard *et al.*, 2021; Slot *et al.*, 2021b). The assumption that g_0 is constant could therefore bias estimations of g_{sw}. A way of testing this assumption is to measure leaf conductance in the dark to minimize stomatal opening and thus better highlight the role of the cuticle in the temperature response.

Here, we explore the following questions using gas exchange observations from five tropical tree species in a seasonally-dry Panamanian forest: (1) Does the response of stomatal conductance to *VPD* depend on whether the increase in *VPD* is driven by increasing temperature or decreasing *RH*? (2) Which stomatal model best represents variation in stomatal conductance associated with changes in RH and temperature? (3) How does the parameter g_0 vary with leaf temperature and RH?

Materials and Methods

Site study and plant material

This study was conducted in Parque Natural Metropolitano (8.9944, -79.5431, elevation 150m) in the Republic of Panama, where the Smithsonian Tropical Research Institute operates a construction crane for accessing the top of the forest canopy. Mean precipitation is 200 mm/month during the rainy season from April to December and 25 mm/month during the dry season (January to March). Mean air temperature is 26 °C with minimum and maximum average temperatures between 23 °C and 32 °C (Paton, 2022). Minimum air RH is rarely below 43 %, and maximum air temperature rarely exceeds 34 °C (less than 0.5 % of the days, Fig. S1). Experiments were conducted in February and March 2022.

We selected upper-canopy branches from five species with different ecological strategies (Table 1). Branches were collected from the crane gondola pre-dawn, and quickly immersed in water and recut several times to avoid xylem cavitation . Branches were then brought down to the ground, where the measurements were performed. This excision protocol allowed us to conduct extended response curves – that are not possible *in situ* due to wind moving the crane gondola – while minimizing the impact of excision on stomatal function (Verryckt *et al.*, 2020; Davidson *et al.*, 2022). Healthy, mature leaves were selected for the measurements of gas exchange response curves to temperature and RH, both in light and dark conditions.

Leaf gas exchange measurements

Gas exchange measurements were performed using two LI-6800 portable photosynthesis systems (LI-COR, Lincoln, NE, USA) equipped with 6 cm^2 chambers (6800-01A) and four LI-6400XT systems (LI-COR, Lincoln, NE, USA) mounted with 2 × 3 cm^2 leaf chambers. We equipped the chambers with polymer gaskets to avoid leaks and used the same light spectrum (90 % red, 10 % blue) for all the instruments. We used the LI-6800 to measure the stomatal response to leaf temperature (T_{leaf}) at fixed relative humidity (*RH*), and we used the LI-6400XT to measure the stomatal response to *RH* at fixed T_{leaf}. At the beginning of each curve, an auto-program logged gas exchange every ten seconds and matched the sample and reference gas analyzer every ten minutes. We averaged the data records for each minute to produce response curves to *RH* and $T_{leaf.}$

For the temperature response curves, we set *RH* at 55 % or 60 %, depending on ambient conditions when we initiated the curves. Air CO_2 concentration at the leaf surface was set to 400 ppm, and the irradiance was set to 400 µmol m^{-2} s^{-1}. This light level was below saturation for all the species and avoided additional heat load from the LI-COR light source and enabled measurements at a low temperature (23 °C). T_{leaf} set points were: 23, 27, 30, 33, 37, and 41 °C. Depending on the conductance value at 41 °C we added one or two additional higher temperature levels up to 46 °C, to reach low photosynthesis and conductance rates, and to approach the minimum conductance at high temperature. For some high-temperature measurements (>= 41 °C), and depending on the ambient conditions, it was not possible to maintain RH constant, as this would have led to condensation inside the instrument. In these cases, *RH* was automatically reduced to a lower level (45 %). For all the temperature levels, measurements were taken only after the conductance and photosynthesis values were stable, as visualized on the instrument display, following a minimum acclimation time of 15 minutes (Fig. S2). Between five and eight temperature response curves were measured for each species.

Gas exchange response curves to RH were performed under the same conditions as the temperature curves. Leaf temperature was set to a constant value between 25 °C and 30 °C, based on the ambient temperature at the beginning of the curves. Relative humidity was controlled by manually adjusting the air flow through the desiccant column. We started the curves at a high RH and decreased it sequentially in four or more steps. The lowest RH that could be reached depended on the leaf transpiration rate, the desiccant freshness, which was

impacted by the measurement duration, and the ambient atmospheric conditions. The highest RH usually did not exceed 80 % to avoid condensation inside the instrument. Between six and eight RH response curves were measured for each species.

We also evaluated the effects of *RH* and T_{leaf} on the dark-adapted conductance ($g_{sw,dark}$). We define the dark-adapted conductance as $g_{sw,dark}$ rather than $g_{0,}$ to avoid ambiguity, as g_0 can have different meanings depending on conductance models (Table 2). To measure $g_{sw,dark}$, we used the same protocols as for light-adapted curves, but we turned the gas exchange instrument light source off and covered the analyzer head with a dark cloth to block diffuse light from reaching the leaf inside the chamber. We waited for a minimum of 20 minutes of dark adaptation before measurements. These measurements were also used to analyze the effect of temperature on the dark-adapted respiration rate (R_{dark}). Four temperature curves were measured in the dark for each species, along with three to six RH curves.

Modeling the steady-state leaf conductance response to temperature and relative humidity

We used Equation 1 to model the steady state g_{sw}, assuming that the dependence on air CO_2 is $f(CO_2) = 1/ CO_2$:

$$g_{sw} = g_0 + 1.6\, g_1 \frac{1}{CO_2} f(A) f(VPD_{leaf}) \quad (2)$$

This $f(CO_2)$ function has been used in many conductance models and was not evaluated in this study since CO_2 was held constant during the measurements (Ball *et al.*, 1987; Medlyn *et al.*, 2011). The added 1.6 constant in Equation 2 derives from the Unified Stomatal Optimization model (USO, Medlyn *et al.*, 2011) and represents the ratio of the diffusivities of water to CO_2 in the air. We kept this constant in Equation 2 to enable comparison of g_1 with previously published datasets (Lin *et al.*, 2015; Wu *et al.*, 2020; Davidson *et al.*, 2023; Slot *et al.*, 2024).

We evaluated the accuracy of two *f(VPD)* and three *f(A)* formulations in simulating the g_{sw} response to T_{leaf} and *RH*. For *f(A)*, we tested a linear dependence on net assimilation (A_n, Ball *et al.*, 1987; Leuning, 1995), a linear dependence on gross assimilation (A_g, Yin & Struik, 2009), and a quadratic dependence on gross assimilation ($A_{g,}^2$ Lamour *et al.*, 2022a). The value A_g is related to A_n through: $A_g = A_n + R_{dark}$, and for each species, we modeled the response of R_{dark} to

T_{leaf} based on R_{dark} measurements (See section "Effect of the temperature on the dark respiration").

We also explored two formulations for *f(VPD)*: the formulation from the USO model (Medlyn *et al.*, 2011), where g_{sw} varies with $1/\sqrt{VP\,D_{leaf}}$, and an alternative formulation, *f(VPD) = RH*, where the conductance does not depend on an explicit function of T_{leaf} at constant *RH* (Ball *et al.*, 1987). Importantly, even if there is no explicit effect of the temperature on g_{sw} in the case where *f(VPD) = RH*, T_{leaf} has an implicit effect on g_{sw} as it impacts *f(A)* in equation 2.

We evaluated the performance of the g_{sw} representation by the 3 × 2 combinations of *f(A)* and *f(VPD)* listed in Table 2, where model 1 in this table corresponds to the USO model, model 2 corresponds to Ball *et al.* (1987) and model 5 corresponds to Lamour *et al.* (2022a). Note that these models all have g_0 expressed in mol m^{-2} s^{-1}, but g_0 corresponds to the leaf dark-adapted conductance ($g_{sw,dark}$) in models where A_g is used and to the leaf conductance at the light compensation point in g_{sw} models where the net assimilation is used (Table 2). g_1 has values and units that depend on the model covariates.

We used a linear mixed effect model to evaluate the effect on g_{sw} of *X*, the regressor of the model, where g_0 and g_1 represent the intercept and the slope of the linear model, respectively (Table 2). Since multiple measurements were made on the same leaves, we considered a random leaf effect on g_0 and g_1, and we modeled the effect of the species on g_0 and g_1 with a fixed effect. Leaves from the same tree were treated as independent samples. We evaluated the performance of the different formulations by analyzing the residuals of the models as well as the Akaike criterion of information (AIC; Akaike, 1974) and the standard deviation of the residual (σ). We also calculated the marginal R^2 (R^2_m) associated with the fixed effects only, and the conditional R^2 (R^2_c) that considers the random leaf effect using the package "MuMIn" (Burnham & Anderson, 2004; Bartoń, 2022). We analyzed the performance of the g_{sw} models in representing combined and separate *RH* and T_{leaf} curves. To assess whether the protocol (*RH* or T_{leaf} curves) impacted g_1, we included the curve type as a fixed effect on g_1.

Effect of temperature on the dark respiration

We modeled the temperature dependence of R_{dark} using an Arrhenius function (Equation 3), which represents an exponential increase of R_{dark} with temperature. We also used an alternative equation that represents a peak before decreasing (Equation 4, Harley & Tenhunen, 1991;

Bernacchi *et al.*, 2003). Both equations scale R_{dark} based on its value at a reference temperature of 25 °C, R_{dark25}, where E_a in kJ mol^{-1} represents the activation energy of R_{dark} with temperature, and H_d and S are respectively the enthalpy of deactivation, and the entropy of the peak function. R is the universal gas constant, T_{leaf} is expressed in Kelvin, and the constant 298.15 corresponds to a reference temperature of 25 °C in Kelvin.

$$R_{dark}(T_{leaf}) = R_{dark25} \exp\left(\frac{E_a}{R298.15} - \frac{E_a}{RT_{leaf}}\right) \quad (3)$$

$$R_{dark}(T_{leaf}) = R_{dark25} \exp\left(\frac{E_a}{R298.15} - \frac{E_a}{RT_{leaf}}\right) \frac{1+\exp\left(\frac{S298.15 - H_d}{R298.15}\right)}{1+\exp\left(\frac{ST_{leaf} - H_d}{RT_{leaf}}\right)} \quad (4)$$

We estimated R_{dark25}, E_a, and H_d for each species using a nonlinear mixed model where the effect of the individual leaf of each temperature curve was modelled as a random factor on R_{dark25}. We examined the residuals of each model as well as the AIC to determine if it was necessary to model a deactivation at high temperatures. We could not determine S and H_d together for lack of data at a temperature above 41 °C so we decided to set S to a fixed value of 0.490 kJ mol^{-1} K^{-1}, as used in some vegetation models (Bonan *et al.*, 2011; Oleson *et al.*, 2013; Koven *et al.*, 2020), and to estimate H_d.

Leaf dark-adapted conductance response to temperature and relative humidity

$g_{sw,dark}$ may change with RH or with T_{leaf} if the stomata still respond in the dark to the evaporative demand or if the cuticular conductance is altered, for example, at high temperature (Schreiber, 2001; Drake *et al.*, 2018; Cochard *et al.*, 2021; Slot *et al.*, 2021b). We tested this assumption by fitting the $g_{sw,dark}$ response curves to RH and T_{leaf} with classical regression models, linear, quadratic, and exponential, equations 5, 6, and 7, respectively. In these equations, $g_{sw,dark}$ was the response variable, and RH or T_{leaf} were the explanatory variables, written as X. The parameters a, b, and c are estimated by the regression. To ensure the intercept a was in the range of the data we collected, we centered the variables RH and T_{leaf} at 80 % and 25 °C, respectively. Therefore, X in equations 5, 6, and 7 represents T_{leaf} – 25 °C or RH – 80 %. We accounted for repetitions within individual leaves by considering a random effect of the leaves on a and b, and we made the

regressions for each species separately. As for the other analyses, we used the package "nlme" in the R environment and evaluated the performance of the models using the AIC and the standard error of the residuals (σ).

$$g_{sw,dark} = a + bX \quad (5)$$

$$g_{sw,dark} = a + bX + c\,X^2 \quad (6)$$

$$g_{sw,dark} = a\,e^{bX} \quad (7)$$

Wrong-way response analysis

We evaluated the change in g_{sw} that followed each perturbation in *VPD*, which we called Δg_{sw}, by comparing the steady-state g_{sw} just before a change in T_{leaf} or *RH* with the g_{sw} two minutes after:

$$\Delta g_{sw} = g_{sw}(t + 2\,min) - g_{sw}(t) \quad (8)$$

Consistent with LI-COR recommendations for conducting gas exchange measurements, we considered that two minutes was long enough to flush air from the chamber of the LI-6400XT and LI-6800 instruments, yet sufficiently short for analyzing the wrong-way response (Buckley *et al.*, 2011).

We tested if Δg_{sw} was significantly different from zero using a t-test with a random effect of the leaf with the package "nlme". A $\Delta g_{sw} > 0$ is interpreted as a WWR when VPD_{leaf} increases. We also tested if Δg_{sw} depended on the steady-state conductance value before the *VPD* increment using a linear mixed model. In this model, we fixed the intercept at 0 mol m^{-2} s^{-1} and included a leaf random effect to account for the multiple observations made on the same leaves.

Impact of the conductance models on leaf-scale gas exchange simulations

We evaluated the impact of the conductance models on simulations of g_{sw} and *A* response to *RH* and T_{leaf}. To achieve this, we coupled the leaf conductance equations (Table 2) with the photosynthesis equations (Farquhar *et al.*, 1980) and solved the resulting system analytically. This reduced the problem to a polynomial of degree 2 or 3, from which we selected the real and biologically sound solution (Baldocchi, 1994; Yin & Struik, 2009; Lamour *et al.*, 2022a). Each conductance model was parameterized with its corresponding g_0 and g_1 values (averaged across the five tree species), as estimated in this study. Additionally, the Farquhar *et al.* (1980) model's

parameters, i.e., the maximum carboxylation capacity (V_{cmax25}), the maximum electron transport rate (J_{max25}), and R_{dark25} were set to 46, 83, and 0.75 μmol m^{-2} s^{-1}, respectively. The V_{cmax25} and J_{max25} values are average values that we measured on the same species during the same campaign (Lamour *et al.*, 2023a). Temperature dependencies for V_{cmax25} and J_{max25} were modeled according to Kumarathunge *et al.* (2019) for plants growing at 26 °C (*i.e.*, the mean average temperature at the study site), while the R_{dark25} temperature dependence was defined using the mean parameters from this study. CO_2 concentration and irradiance were held constant at 400 ppm and 400 μmol m^{-2} s^{-1}, respectively. *RH* was set to 55 % when investigating T_{leaf} effects, and T_{leaf} was set to 28 °C for exploring *RH* effects.

Results

Comparison of steady-state models of conductance

Figure 1 shows the responses of A and g_{sw} to changes in VPD_{leaf} achieved by modifying T_{leaf} between 23 °C and up to 46 °C and *RH* between 73.9 ± 5.9 % and 28.5 ± 8.8 % at the driest level. The *RH* manipulation produced a markedly narrower range of VPD_{leaf} (1.0 – 2.8 kPa) than when T_{leaf} varied (1.2 – 4.5 kPa).

Despite considerable leaf to leaf variation in g_{sw} and A_n, all six models predicted the leaf conductance response to VPD_{leaf} with good accuracy (R^2_c = 0.85 – 0.94, Fig. 2, Table S1). The error (σ) ranged from 0.017 to 0.025 mol m^{-2} s^{-1}, representing a 40% difference between the lowest and best fit. Nonetheless, comparison of g_{sw} model performance revealed that the A_g^2 and *RH* functions best represented the data (lowest AIC, highest R_c^2, Fig. 2, Table S1). This result was consistent when we considered the T_{leaf} and *RH* response curves separately (Figs S3 and S4, Tables S2 and S3), although the difference between models was less marked when T_{leaf} was constant and *RH* varied (Table S3). Notably, all models overestimated g_{sw} at low *VPD* for *RH* above 65 % and showed a systematic non-zero trend in their residuals (Fig. S5).

Curve type significantly impacted g_1 estimates ($P < 0.02$), with T_{leaf} curves yielding between 17 % and 35 % higher g_1 values than the *RH* curves (Tables S1, S2 and S3). The effect on g_1 disappeared ($P > 0.27$ for all models) when we restricted observations to a *RH* below 65 %, the RH threshold at which all models had a non-zero trend in their residuals (Table S4).

Species significantly impacted g_0 for all models ($P < 10^{-4}$), especially because *C. candidissimum* minimum conductance was exceptionally high, consistent with our results on $g_{sw,dark}$ (see "*Response of dark-acclimated conductance to temperature and relative humidity*"). For g_1, the species effect was significant ($P < 0.02$, Table S4) for models using the A_g and A_n covariates. However, the species had the same g_1 for models using A_g^2 (non-significant effect on g_1, $P > 0.15$, Table S4).

Response of dark-acclimated conductance and respiration to temperature and relative humidity

R_{dark} varied between 0.36 and 1.07 µmol m^{-2} s^{-1} at 23 °C and between 1.22 and 3.95 µmol m^{-2} s^{-1} at a high temperature above 41 °C. The peak-shaped function was a better fit to the data than the Arrhenius function (Table 3), even though R_{dark} did not decrease at high temperature. The Peaked function had a better AIC (Table 3) than the Arrhenius function, and the residuals were not biased (Fig. S7).

We tested if $g_{sw,dark}$ was impacted by changes in T_{leaf} and *RH* by fitting linear, quadratic, and exponential models (Fig. 5, Table S5). The response of $g_{sw,dark}$ to T_{leaf} differed among species (Fig. 5a and Table S5). $g_{sw,dark}$ was constant for *C. cainito*, decreased at high temperatures for *C. candidissimum* and *L. seemannii,* and increased in *C. triplinerve* and *D. morototoni*. The response of $g_{sw,dark}$ to changes in *RH* was also species-specific (Fig. 5b and Table S5). $g_{sw,dark}$ was constant for *C. triplinerve,* whereas it decreased with higher *RH* in the other species. $g_{sw,dark}$ was exceptionally high for *C. candidissimum* (Fig. 5b), consistent with the observations made during the $g_{sw,dark}$ response to T_{leaf} (Fig. 5a) as well as in the g_{sw} response curves (Fig. 2).

Wrong way response analysis

Leaf conductance responded dynamically to step changes in T_{leaf} (Fig. S2a). Each modification of T_{leaf} rapidly impacted $g_{sw,}$ which increased at low T_{leaf} and decreased at high T_{leaf}. The time for g_{sw} to stabilize after a step change in T_{leaf} took tens of minutes, after sometimes overshooting, i.e., reaching a value higher or lower than the final steady-state g_{sw} (Fig. S2a). In *D. morototoni*, g_{sw} often oscillated after a change in T_{leaf} (Fig. S6). Changes in T_{leaf} did not create an apparent wrong-way response, and the g_{sw} data remained temporally continuous (Fig. S2a). The absence of a WWR was confirmed statistically for the overall dataset, and Δg_{sw} was not significantly different from zero (Δg_{sw} = + 0.002 ± 0.004 SE mol m^{-2} s^{-1}, $P = 0.6$, Fig. 3a).

In contrast to T_{leaf} response curves, an immediate (< 2 min) increase in g_{sw} followed a decrease in *RH* in the leaf chamber (Δg_{sw} = + 0.02 ± 0.01 SE mol m^{-2} s^{-1}, $P < 10^{-9}$, Fig. 3b). This WWR was species-dependent ($P < 2.10^{-4}$). *C. cainito* showed no increase (Δg_{sw} =+ 0.00 ± 0.01 SE, $P = 0.5$, Fig. 3b) whereas *D. morototoni* showed the largest increase (Δg_{sw} = + 0.04 ± 0.01 SE, $P < 10^{-8}$, Fig. 3b). The quick increase in g_{sw} after a change in *RH* was not followed by a marked decrease in g_{sw} between the first level of *RH* above 70 % and the second level above 55 %. As a result, the steady-state g_{sw} remained constant between these two *RH* levels (*C. cainito*: - 0.015 ± 0.022 SE, $P = 0.29$; *C. candidissimum*: + 0.011 ± 0.012 SE, $P = 0.27$) or even increased (*L. seemannii:* + 0.023 ± 0.01 SE, $P = 0.02$; *C. triplinerve*: + 0.017 ± 0.006 SE, $P = 0.02$) which explained the trend in the residuals of the models (Fig. S5) since all the models we compared predicted a decrease in steady-state g_{sw} when *RH* decreased (Table 2).

We also tested if the WWR depended on the steady-state g_{sw} just before the change in *RH*. We found that WWR depended on g_{sw} (Fig. 4, $P < 10^{-4}$). The slope of the relationship depended on the species ($P < 10^{-4}$) and was not significantly different from 0 in *C. cainito*.

Consistent with the WWR results in the light, in the dark, we did not find evidence that variation in leaf temperature created a WWR (Δg_{sw} = 0. 00 ± 0.00 SE mol m^{-2} s^{-1}, $P = 0.8$, Fig. 4a, Dark), whereas we did find evidence that the changes in *RH* created a WWR (Δg_{sw} = + 0.01 ± 0.00 SE mol m^{-2} s^{-1}, $P < 10^{-16}$, Fig. 5b, Dark). In contrast with the WWR in the light, the WWR in the dark was not species dependent at a 0.05 P-value threshold ($P = 0.06$).

Impact of the conductance models on steady-state leaf-scale gas exchange simulations

We compared the *RH* and T_{leaf} responses of the models proposed by Medlyn *et al.* (2011) and Ball *et al.* (1987) with the best-fit model from this study (Fig. 6). In simulations, since the effect of *RH* and T_{leaf} on $g_{sw,dark}$ was moderate and inconsistent across species, we considered that g_0 was a constant. The simulated response of g_{sw} to changes in T_{leaf} differed among the three models (Fig. 6a). Notably, the best-fit model demonstrated a greater stomatal sensitivity to changes in T_{leaf} compared to the Medlyn *et al.* (2011) and Ball *et al.* (1987) models. The Medlyn *et al.* (2011) model simulated an optimal temperature of 18.7 °C for g_{sw}, whereas the Ball *et al.*, (1987) and best-fit models simulated optimal temperatures of 28.0 °C and 30.2 °C, respectively.

The choice of the model also impacted the optimum temperature for A. The optimal temperature was 26.7°C, 28°C, and 28.6°C for Medlyn *et al.* (2011), Ball *et al.* (1987), and the best fit model, respectively. The g_{sw} response predicted by the Medlyn *et al.* (2011) model departed markedly from the other models at high *RH* and low *RH*. The conductance model affected the prediction of A under varying *RH* conditions (Fig. 6d) but had a smaller impact on A when T_{leaf} changed (Fig. 6c). For *RH* values below 50 %, the Medlyn *et al.* (2011) model simulated A rates almost double those simulated by the other models.

Discussion

An accurate representation of the effect of *VPD* on stomatal conductance is central to improved prediction of the effect of a changing climate on tropical forests. In the present study, we examined the physiological response of leaves to increasing *VPD* driven by either increasing temperature or decreasing *RH,* and compared six steady-state conductance model formulations that differed in their representation of the effect of photosynthesis and evaporative demand. We observed distinct responses of g_{sw} to changes in *VPD* induced by manipulating *RH* or $T_{leaf,}$. The stomatal parameter g_1 was higher when estimated using g_{sw}-T_{leaf} response curves compared to estimates from g_{sw}-*RH* response curves, showing a lower stomatal sensitivity to *RH* changes. In addition, and contrary to our expectations, the wrong-way response of stomata was observed following a change in *RH* but not following a temperature change (Fig. 3). Our comparison of empirical stomatal models showed that using a nonlinear effect of photosynthetic rate (A_g^2) and *RH* instead of VPD_{leaf} better represented the response of g_{sw} to A and *VPD* (Fig. 2). This result was consistent when *VPD* was increased by raising the temperature at constant *RH* or when *RH* was lowered at constant temperature. Importantly, all models overestimated g_{sw} at high *RH. W*e showed that *VPD* had a negligible effect on conductance in the dark (Fig. 5) in the range of temperature we used, suggesting that cuticle properties played no role in the observed conductance response to *VPD* and that the assumption of a constant g_0 is not a major source of uncertainty in conductance models for this site.

Distinct effect of temperature and relative humidity on the stomatal response to VPD

In this study, we varied leaf temperature between 23 and 46°C. These leaf temperatures are realistic for this type of forest, although 46°C is at the high end of the leaf temperature distribution in tropical forests (Rey-Sánchez *et al.*, 2016; Doughty *et al.*, 2023). These temperature variations had a more significant impact on the VPD than when we modified *RH* at ambient temperature. In these conditions, we observed that modifying T_{leaf} or *RH* produced a different stomatal response. The stomatal sensitivity parameter (g_1) was lower when estimated from *RH* response curves compared to T_{leaf} curves. This indicates a lower stomatal sensitivity when *RH* changes, which can be partly explained by the behavior we observed at very high *RH* (Fig. S5). In that case, decreasing *RH* tended to increase leaf conductance, a phenomenon not explained by most stomatal conductance models. A similar observation was made in some tropical species in Brazil (Domingues *et al.*, 2014) and in other ecosystems (Eamus & Cole, 1997; Eamus *et al.*, 2008). The analysis of the WWR suggests that the rapid increase in leaf conductance associated with the decrease in *RH* was not followed by the expected decrease in g_{sw} (the "right way response"). This absence of a proportional right-way response suggests that the threshold *RH* for activating a stronger stomatal closure may not have been reached, or that its timescale exceeded our observation window.

Importantly, we observed significant WWR when VPD_{leaf} changed with *RH*, but not T_{leaf}. The WWR that follows a change in VPD_{leaf} is thought to occur due to a passive reaction of stomata to a change in turgor in the epidermal cells (Buckley, 2019). This is explained by changes in cuticular transpiration, which causes the epidermal cells to swell or contract, thereby mechanically influencing stomata opening. This passive effect is also linked to the turgor of guard cells. Open stomata are more susceptible to changes in the leaf epidermal turgor than closed and flaccid stomata (Buckley, 2019). This is visible in the data with a positive correlation between Δg_{sw} and steady-state g_{sw} (Fig. 4). However, the absence of WWR during the T_{leaf} response curves, in the dark or at 400 µmol m^{-2} s^{-1} irradiance is intriguing as we would have expected an increase in VPD_{leaf} caused by an increase in T_{leaf} to also create a WWR, similarly to what happened when *RH* changed. It has been shown that the cuticle swells or shrinks depending on air *RH*, which is a result of changes in cuticle water sorption (Chamel *et al.*, 1991, 1992; Fernández *et al.*, 2017), a process that is independent of VPD_{leaf} and T_{leaf} (Kerstiens, 1996; Tredenick & Farquhar, 2021). However, it is unclear whether the shrinkage of the cuticle with *RH* could significantly impact stomata aperture. If changes in the cuticle volume impact stomata aperture, it could explain the wrong-way response observed, significant with *RH* but not T_{leaf}.

Note, that the common assumption is that the epidermal cell turgor affects the dynamics of the guard cells and not the epidermal cuticle volume.

Representing the effect of leaf temperature and air relative humidity on stomatal steady-state conductance

Among the leaf conductance models tested in this study, the formulations that included A_g^2 better represented g_{sw} measurements than models adopting a linear formulation. Moreover, using this formulation, g_1 was similar across species, simplifying the parametrization of the model, a similar result to that obtained in Amazonian tree species (Lamour *et al.*, 2023b).

Many empirical models use *f(A)* as a covariate (Damour et al. 2010). Compared to the other environmental variables of Equation 1, *f(A)* is a physiological variable that depends on multiple biochemical properties of the leaf and responds to other environmental variables such as light and temperature. The use of *f*(*A*) dramatically simplifies the study of stomatal conductance and has proven highly effective for applications in ecophysiology. However, this approach requires a model of photosynthesis for predicting new rates based solely on environmental conditions, a process in which *f(A)* also needs to be simulated (Fig. 6, Damour *et al.*, (2010)). However, the use of *f(A)* holds some level of circularity since A_n itself is impacted by g_{sw} through the supply of CO_2. This circularity is likely to inflate the seemingly good performance of the models (R^2_c = 0.85 - 0.94). We propose that the considerable within-leaf and between-leaf variability in g_{sw} (Fig. 1) derives from a high variability in the photosynthetic properties of the leaves (for example V_{cmax25}, J_{max25}, R_{day25}, etc.), which is accounted for by the use of *f(A)* in all the models we tested.

For representing *f(A)*, most empirical models use a linear relationship between A_n or A_g and g_{sw} (Ball *et al.*, 1987; Leuning, 1995; Yin & Struik, 2009; Damour *et al.*, 2010; Medlyn *et al.*, 2011; Prentice *et al.*, 2014) but several studies have shown that this relationship is not linear when the irradiance varies (Ball, 1988; Barnard & Bauerle, 2013; Busch, 2014; Lamour *et al.*, 2022a; Xue *et al.*, 2024). Here, we showed that accounting for this nonlinearity also improved the goodness of fit when *RH* and T_{leaf} varied at constant irradiance (Fig. 2), and therefore confirmed the benefit of a nonlinear formulation over a wider range of environmental conditions. The non-

linear relationship between A and g_{sw} suggests that stomatal conductance responds more strongly to temperature than the gradual response predicted by linear models (Fig. 6).

When T_{leaf} varied, models that used *RH* in their formulation performed better than those models using $1/\sqrt{VPD_{leaf}}$. The relative humidity was held constant (55 ± 3 % SD) during the measurement of the T_{leaf} curves, which implies that accounting for the T_{leaf} effect on A was sufficient to model the leaf temperature effect on g_{sw}.

When *RH* varied, the choice of the formulation didn't dramatically impact the model fits. Nonetheless, models using *RH* fitted the observations slightly better than models using $1/\sqrt{VPD_{leaf}}$. The weak sensitivity of g_{sw} at high *RH* could explain the slightly improved accuracy of the *RH* formulation over $1/\sqrt{VPD_{leaf}}$ as this latter formulation diverges as VPD_{leaf} tends to zero (Xue *et al.*, 2024). Specifically, in models using $1/\sqrt{VPD_{leaf}}$, g_{sw} is predicted to be high at low VPD_{leaf} and is more sensitive to decreasing *RH* than the g_{sw} models based directly on *RH* (Fig. 6). Furthermore, at high values of VPD_{leaf}, models using $1/\sqrt{VPD_{leaf}}$ predict nearly invariant g_{sw} with increasing VPD_{leaf} whereas models using *RH* in their formulation simulate a decrease (Franks *et al.*, 2017; Li *et al.*, 2022, Fig. 6) and could also explain the better accuracy of the *RH* formulation.

The model choice significantly impacted the simulated optimal temperature for g_{sw} and A. This finding highlights a key uncertainty: accurately representing stomatal behavior is vital for determining if tropical forests are close to a temperature threshold (Doughty *et al.*, 2023). Modeling stomatal conductance is central to using Earth System Models to project atmosphere - vegetation feedbacks. A fundamental issue is that most empirical and optimal equations are developed and validated using short-term (hourly or daily) data. Over longer timescales (years to decades), shifting environmental conditions are likely to impact many properties of the leaves such as their composition, anatomy and function (López *et al.*, 2021). As a consequence, g_0, g_1, and the parameters governing *f(A)* such as V_{cmax25} or J_{max25} are also expected to vary. Therefore, the long-term response of g_{sw} may not be accurately predicted by the instantaneous function of the environment predicted in short term models (Equation 1, Fig. 6).

Effect of relative humidity and leaf temperature on $g_{sw,dark}$

For all the species except *C. candidissimum*, the effect of T_{leaf} on $g_{sw,dark}$ was moderate or non-significant within the temperature range defined in this study. In a previous comparative study of the leaf cuticular conductance of 24 tropical species, it was found that temperature did not affect the cuticular conductance in 17 species within a temperature range of 25 °C to 50 °C. Of the seven species that showed an increase in cuticular conductance at high T_{leaf}, the increase started on average at 42 °C (Slot *et al.*, 2021b). The increase in $g_{sw,dark}$ that we measured also occurred above 40 °C for *D. morototoni* and *C. triplinerve*. It should be noted that it was not possible to increase the leaf temperature above 40 to 46 °C in our study, due to the need to avoid condensation issues in the gas-exchange instrument.

C. candidissimum showed surprising behavior with an exceptionally high conductance in the dark, although not unprecedented in other species (Caird *et al.*, 2007; Barbour & Buckley, 2007). In all the measurements performed (g_{sw} and $g_{sw,dark}$ response to T_{leaf} and *RH,* Fig. 2 and Fig. 5) this species had a high minimum conductance, which suggests that this is not an artefact of the measurement. A likely explanation is that the stomata were not closed or that the cuticle was relatively more permeable than in the other species.

RH had a small effect on $g_{sw,dark}$ in three out of the five species. This could be due to sensitive stomata in the dark, as was found for *Ricinus communis* (Barbour & Buckley, 2007) or to a cuticular response at low relative humidity (Boyer *et al.*, 1997; Schreiber *et al.*, 2001; Boyer, 2015).

The $g_{sw,dark}$ varied greatly across species, with a five-fold difference between *C. triplinerve* and *L. seemannii* at 25 °C, and a forty-fold difference if *C. candidissimum* is included in the comparison (Table S5), close to the thirty-fold difference in cuticular conductance found by Slot *et al.* (2021). Given the importance of night-time transpiration (Caird *et al.*, 2007; Lombardozzi *et al.*, 2017) as well as minimum conductance in the species vulnerability to drought (Martin-StPaul *et al.*, 2017; Choat *et al.*, 2018), understanding the species difference in $g_{sw,dark}$ is important for modeling purposes. However, the assumption that g_0 is a constant of environmental conditions, especially T_{leaf} and *RH* was a small source of uncertainty in this study compared to the species effect.

Conclusions

Stomata play a key role in controlling gas exchange, yet their function remains a major source of uncertainty in Earth system models, and their equations are still largely empirical. They remain poorly tested in the tropics due to the difficulty of accessing the top of the tree canopy and the duration of gas exchange measurements. In this study, we compared several stomatal conductance models that differ in their representation of the effect of temperature and relative humidity. We showed that the response to relative humidity is poorly represented in current models, especially at high relative humidity levels. This bias could have a profound impact on estimates of both transpiration and the primary productivity of tropical forests. Furthermore, the estimation of stomatal parameters depended on the measurement protocol, complicating the comparison of stomatal traits across studies and environments. While the compared conductance models had fairly similar performance, the choice of model impacted simulated conductance at the extremes of the temperature and relative humidity ranges and affected the simulated thermal optimum of photosynthesis. This shows the importance of improving stomatal theory to understand tropical ecosystem responses to climate change. Finally, our data did not support an increase in leaf conductance under high-temperature conditions in the dark. Therefore, we conclude that the hypothesis of a constant cuticular conductance was not a major source of uncertainty in the range of temperature that we used compared to the other uncertainties related to stomatal function.

Authors' contributions

JL, KD: data collection and curation; AR, JL, KD, SS: conceptualization and methodology; JL: formal analysis and writing of the original draft; AR, JC, MS, JL, KD, SS: writing - review & editing.

Acknowledgements

We are grateful to the staff of the STRI for assistance with field logistics and to Edwin Andrades for operating the canopy crane. We thank Tom Buckley for valuable discussion.

Funding

This work was supported by the Next Generation Ecosystem Experiments-Tropics project funded by the US Department of Energy, Office of Science, Office of Biological and Environmental Research and by U.S. Department of Energy Contract No. DE-AC02-05CH11231 to Lawrence Berkeley National Laboratory.

Data availability

The data that support the findings of this study are openly available in the NGEE Tropics Data Collection at https://doi.org/10.15486/ngt/1896884, reference number NGT0192 (Lamour *et al.*, 2023a). The processed data used to produce Fig. 2 and Fig. 5 are included as supplementary files.

References

Ainsworth EA, Rogers A. **2007**. The response of photosynthesis and stomatal conductance to rising [CO2]: mechanisms and environmental interactions. *Plant, Cell & Environment* **30**: 258–270.

Akaike H. **1974**. A new look at the statistical model identification. *IEEE transactions on automatic control* **19**: 716–723.

Baldocchi D. **1994**. An analytical solution for coupled leaf photosynthesis and stomatal conductance models. *Tree Physiology* **14**: 1069–1079.

Ball JT. **1988**. An analysis of stomatal conductance.

Ball JT, Woodrow IE, Berry JA. **1987**. A Model Predicting Stomatal Conductance and its Contribution to the Control of Photosynthesis under Different Environmental Conditions. In: Biggins J, ed. Progress in Photosynthesis Research: Volume 4 Proceedings of the VIIth International Congress on Photosynthesis Providence, Rhode Island, USA, August 10–15, 1986. Dordrecht: Springer Netherlands, 221–224.

Barbour MM, Buckley TN. **2007**. The stomatal response to evaporative demand persists at night in Ricinus communis plants with high nocturnal conductance. *Plant, Cell & Environment* **30**: 711–721.

Barnard DM, Bauerle WL. **2013**. The implications of minimum stomatal conductance on modeling water flux in forest canopies. *Journal of Geophysical Research: Biogeosciences* **118**: 1322–1333.

Bartoń K. **2022**. *MuMIn: Multi-Model Inference*.

Bernacchi CJ, Pimentel C, Long SP. **2003**. In vivo temperature response functions of parameters required to model RuBP-limited photosynthesis. *Plant, Cell & Environment* **26**: 1419–1430.

Bonan GB, Lawrence PJ, Oleson KW, Levis S, Jung M, Reichstein M, Lawrence DM, Swenson SC. **2011**. Improving canopy processes in the Community Land Model version 4 (CLM4) using global flux fields empirically inferred from FLUXNET data. *Journal of Geophysical Research* **116**.

Boyer JS. **2015**. Turgor and the transport of CO2 and water across the cuticle (epidermis) of leaves. *Journal of Experimental Botany* **66**: 2625–2633.

Boyer JS, Wong SC, Farquhar GD. **1997**. CO2 and water vapor exchange across leaf cuticle (epidermis) at various water potentials. *Plant physiology* **114**: 185–191.

Brando PM, Barlow J, Macedo MN, Silvério DV, Ferreira JN, Maracahipes L, Anderson L, Morton DC, Alencar A, Paolucci LN, *et al.* 2025. Tipping Points of Amazonian Forests: Beyond Myths and Toward Solutions. *Annual Review of Environment and Resources* **50**: 97–131.

Brodribb TJ, Powers J, Cochard H, Choat B. **2020**. Hanging by a thread? Forests and drought. *Science* **368**: 261–266.

Buckley TN. **2016**. Stomatal responses to humidity: has the 'black box' finally been opened? *Plant, Cell & Environment* **39**: 482–484.

Buckley TN. **2019**. How do stomata respond to water status? *New Phytologist* **224**: 21–36.

Buckley TN, Mott KA, Farquhar GD. **2003**. A hydromechanical and biochemical model of stomatal conductance. *Plant, Cell & Environment* **26**: 1767–1785.

Buckley TN, Sack L, Gilbert ME. **2011**. The Role of Bundle Sheath Extensions and Life Form in Stomatal Responses to Leaf Water Status. *Plant Physiology* **156**: 962–973.

Burnham KP, Anderson DR (Eds). **2004**. *Model Selection and Multimodel Inference*. Springer New York.

Busch FA. **2014**. Opinion: The red-light response of stomatal movement is sensed by the redox state of the photosynthetic electron transport chain. *Photosynthesis Research* **119**: 131–140.

Byrne MP, O'Gorman PA. **2016**. Understanding Decreases in Land Relative Humidity with Global Warming: Conceptual Model and GCM Simulations. *Journal of Climate* **29**: 9045–9061.

Caird MA, Richards JH, Donovan LA. **2007**. Nighttime Stomatal Conductance and Transpiration in C3 and C4 Plants. *Plant Physiology* **143**: 4–10.

Chamel A, Escoubes M, Baudrand G, Girard G. **1992**. Determination of water sorption by cuticles isolated from fir tree needles. *Trees* **6**: 109–114.

Chamel A, Pineri M, Escoubes M. 1991. Quantitative determination of water sorption by plant cuticles. *Plant, Cell & Environment* **14**: 87–95.

Choat B, Brodribb TJ, Brodersen CR, Duursma RA, López R, Medlyn BE. 2018. Triggers of tree mortality under drought. *Nature* **558**: 531–539.

Cochard H, Pimont F, Ruffault J, Martin-StPaul N. 2021. SurEau: a mechanistic model of plant water relations under extreme drought. *Annals of Forest Science* **78**: 55.

Collatz GJ, Ball JT, Grivet C, Berry JA. 1991. Physiological and environmental regulation of stomatal conductance, photosynthesis and transpiration: a model that includes a laminar boundary layer. *Agricultural and Forest Meteorology* **54**: 107–136.

Damour G, Simonneau T, Cochard H, Urban L. 2010. An overview of models of stomatal conductance at the leaf level. *Plant, Cell & Environment* **33**: 1419–1438.

Davidson KJ, Lamour J, Rogers A, Ely KS, Li Q, McDowell NG, Pivovaroff AL, Wolfe BT, Wright SJ, Zambrano A, *et al.* 2023. Short-term variation in leaf-level water use efficiency in a tropical forest. *New Phytologist* **237**: 2069–2087.

Davidson KJ, Lamour J, Rogers A, Serbin SP. 2022. Late-day measurement of excised branches results in uncertainty in the estimation of two stomatal parameters derived from response curves in Populus deltoides Bartr. × Populus nigra L. *Tree Physiology* **42**: 1377–1395.

Domingues TF, Martinelli LA, Ehleringer JR. 2014. Seasonal patterns of leaf-level photosynthetic gas exchange in an eastern Amazonian rain forest. *Plant Ecology & Diversity* **7**: 189–203.

Doughty CE, Keany JM, Wiebe BC, Rey-Sanchez C, Carter KR, Middleby KB, Cheesman AW, Goulden ML, da Rocha HR, Miller SD, *et al.* 2023. Tropical forests are approaching critical temperature thresholds. *Nature* **621**: 105–111.

Drake JE, Tjoelker MG, Vårhammar A, Medlyn BE, Reich PB, Leigh A, Pfautsch S, Blackman CJ, López R, Aspinwall MJ, *et al.* 2018. Trees tolerate an extreme heatwave via sustained transpirational cooling and increased leaf thermal tolerance. *Global Change Biology* **24**: 2390–2402.

Duursma RA, Blackman CJ, Lopéz R, Martin-StPaul NK, Cochard H, Medlyn BE. 2019. On the minimum leaf conductance: its role in models of plant water use, and ecological and environmental controls. *New Phytologist* **221**: 693–705.

Eamus D, Cole S. 1997. Diurnal and Seasonal Comparisons of Assimilation, Phyllode Conductance and Water Potential of Three Acacia and One Eucalyptus Species in the Wet–Dry Tropics of Australia. *Australian Journal of Botany* **45**: 275–290.

Eamus D, Taylor DT, Macinnis-ng CMO, Shanahan S, De Silva L. 2008. Comparing model predictions and experimental data for the response of stomatal conductance and guard cell turgor to manipulations of cuticular conductance, leaf-to-air vapour pressure difference and temperature: feedback mechanisms are able to account for all observations. *Plant, Cell & Environment* **31**: 269–277.

Fang Z, Zhang W, Brandt M, Abdi AM, Fensholt R. **2022**. Globally Increasing Atmospheric Aridity Over the 21st Century. *Earth's Future* **10**: e2022EF003019.

Farquhar GD, Caemmerer von S, Berry JA. **1980**. A biochemical model of photosynthetic CO2 assimilation in leaves of C3 species. *Planta* **149**: 78–90.

Fernández V, Bahamonde HA, Javier Peguero-Pina J, Gil-Pelegrín E, Sancho-Knapik D, Gil L, Goldbach HE, Eichert T. **2017**. Physico-chemical properties of plant cuticles and their functional and ecological significance. *Journal of Experimental Botany* **68**: 5293–5306.

Franks PJ, Adams MA, Amthor JS, Barbour MM, Berry JA, Ellsworth DS, Farquhar GD, Ghannoum O, Lloyd J, McDowell N, *et al.* 2013. Sensitivity of plants to changing atmospheric CO2 concentration: from the geological past to the next century. *New Phytologist* **197**: 1077–1094.

Franks PJ, Berry JA, Lombardozzi DL, Bonan GB. **2017**. Stomatal Function across Temporal and Spatial Scales: Deep-Time Trends, Land-Atmosphere Coupling and Global Models. *Plant Physiology* **174**: 583–602.

Grossiord C, Buckley TN, Cernusak LA, Novick KA, Poulter B, Siegwolf RTW, Sperry JS, McDowell NG. **2020**. Plant responses to rising vapor pressure deficit. *New Phytologist* **226**: 1550–1566.

Harley PC, Tenhunen JD. **1991**. Modeling the Photosynthetic Response of C3 Leaves to Environmental Factors. In: CSSA Special Publications. Modeling Crop Photosynthesis—from Biochemistry to Canopy. 17–39.

Kerstiens G. **1996**. Cuticular water permeability and its physiological significance. *Journal of Experimental Botany* **47**: 1813–1832.

Koven CD, Knox RG, Fisher RA, Chambers JQ, Christoffersen BO, Davies SJ, Detto M, Dietze MC, Faybishenko B, Holm J, *et al.* 2020. Benchmarking and parameter sensitivity of physiological and vegetation dynamics using the Functionally Assembled Terrestrial Ecosystem Simulator (FATES) at Barro Colorado Island, Panama. *Biogeosciences* **17**: 3017–3044.

Kromdijk J, Głowacka K, Long SP. **2019**. Predicting light-induced stomatal movements based on the redox state of plastoquinone: theory and validation. *Photosynthesis Research* **141**: 83–97.

Kumarathunge DP, Medlyn BE, Drake JE, Tjoelker MG, Aspinwall MJ, Battaglia M, Cano FJ, Carter KR, Cavaleri MA, Cernusak LA, *et al.* 2019. Acclimation and adaptation components of the temperature dependence of plant photosynthesis at the global scale. *New Phytologist* **222**: 768–784.

Lamour J, Davidson KJ, Calderón O, Ely KS. **2023a**. Leaf gas exchange and fitted parameters, two sites in Panama, 2022 (v 1.0). Accessed at https://doi.org/10.15486/ngt/1896884.

Lamour J, Davidson KJ, Ely KS, Le Moguédec G, Leakey ADB, Li Q, Serbin SP, Rogers A. **2022a**. An improved representation of the relationship between photosynthesis and stomatal conductance leads to more stable estimation of conductance parameters and improves the goodness-of-fit across diverse data sets. *Global Change Biology* **28**: 3537–3556.

Lamour J, Davidson KJ, Ely KS, Li Q, Serbin SP, Rogers A. **2022b**. New calculations for photosynthesis measurement systems: what's the impact for physiologists and modelers? *New Phytologist* **233**: 592–598.

Lamour J, Souza DC, Gimenez BO, Higuchi N, Chave J, Chambers J, Rogers A. **2023b**. Wood-density has no effect on stomatal control of leaf-level water use efficiency in an Amazonian forest. *Plant, Cell & Environment* **46**: 3806–3821.

Lawson T, Matthews J. **2020**. Guard Cell Metabolism and Stomatal Function. *Annual Review of Plant Biology* **71**: 273–302.

Leuning R. **1995**. A critical appraisal of a combined stomatal-photosynthesis model for C3 plants. *Plant, Cell & Environment* **18**: 339–355.

Li Q, Serbin SP, Lamour J, Davidson KJ, Ely KS, Rogers A. **2022**. Implementation and evaluation of the unified stomatal optimization approach in the Functionally Assembled Terrestrial Ecosystem Simulator (FATES). *Geoscientific Model Development* **15**: 4313–4329.

Lin Y-S, Medlyn BE, Duursma RA, Prentice IC, Wang H, Baig S, Eamus D, de Dios VR, Mitchell P, Ellsworth DS, *et al.* 2015. Optimal stomatal behaviour around the world. *Nature Climate Change* **5**: 459–464.

Lloyd J, Farquhar GD. **2008**. Effects of rising temperatures and [CO2] on the physiology of tropical forest trees. *Philosophical Transactions of the Royal Society B: Biological Sciences* **363**: 1811–1817.

Lombardozzi DL, Zeppel MJB, Fisher RA, Tawfik A. **2017**. Representing nighttime and minimum conductance in CLM4.5: global hydrology and carbon sensitivity analysis using observational constraints. *Geoscientific Model Development* **10**: 321–331.

López J, Way DA, Sadok W. **2021**. Systemic effects of rising atmospheric vapor pressure deficit on plant physiology and productivity. *Global Change Biology* **27**: 1704–1720.

Márquez DA, Stuart-Williams H, Farquhar GD. **2021**. An improved theory for calculating leaf gas exchange more precisely accounting for small fluxes. *Nature Plants* **7**: 317–326.

Martin-StPaul N, Delzon S, Cochard H. **2017**. Plant resistance to drought depends on timely stomatal closure. *Ecology Letters* **20**: 1437–1447.

McAdam SAM, Sussmilch FC, Brodribb TJ. **2016**. Stomatal responses to vapour pressure deficit are regulated by high speed gene expression in angiosperms. *Plant, Cell & Environment* **39**: 485–491.

McDowell N, Allen CD, Anderson-Teixeira K, Brando P, Brienen R, Chambers J, Christoffersen B, Davies S, Doughty C, Duque A, *et al.* 2018. Drivers and mechanisms of tree mortality in moist tropical forests. *New Phytologist* **219**: 851–869.

Medlyn BE, Duursma RA, Eamus D, Ellsworth DS, Prentice IC, Barton CVM, Crous KY, De Angelis P, Freeman M, Wingate L. 2011. Reconciling the optimal and empirical approaches to modelling stomatal conductance. *Global Change Biology* **17**: 2134–2144.

Monteith JL. 1995. A reinterpretation of stomatal responses to humidity. *Plant, Cell & Environment* **18**: 357–364.

Mott KA, Parkhurst DF. 1991. Stomatal responses to humidity in air and helox. *Plant, Cell & Environment* **14**: 509–515.

Mu Y, Hu Y, Jones C, Biggs T, Domingues TF, Funk C, Peterson P. 2025. Increasing dry-season vapor pressure deficit in the Amazon Basin: historical trends, future projections, and links to deforestation. *Environmental Research Communications* **7**: 101001.

Oleson K, Lawrence D, Bonan G, Drewniak B, Huang M, Koven C, Levis S, Li F, Riley W, Subin Z, *et al.* 2013. Technical description of version 4.5 of the Community Land Model (CLM)(No. NCAR/TN-503+ STR). *UCAR: Boulder, CO, USA*.

Paton S. 2022. Monthly summary San Lorenzo crane. Accessed at https://doi.org/10.25573/data.10059518.v28.

Prentice IC, Dong N, Gleason SM, Maire V, Wright IJ. 2014. Balancing the costs of carbon gain and water transport: testing a new theoretical framework for plant functional ecology. *Ecology Letters* **17**: 82–91.

Reich PB, Hobbie SE. 2013. Decade-long soil nitrogen constraint on the CO2 fertilization of plant biomass. *Nature Climate Change* **3**: 278–282.

Rey-Sánchez A, Slot M, Posada J, Kitajima K. 2016. Spatial and seasonal variation in leaf temperature within the canopy of a tropical forest. *Climate Research* **71**: 75–89.

Schreiber L. 2001. Effect of temperature on cuticular transpiration of isolated cuticular membranes and leaf discs. *Journal of Experimental Botany* **52**: 1893–1900.

Schreiber L, Skrabs M, Hartmann K, Diamantopoulos P, Simanova E, Santrucek J. 2001. Effect of humidity on cuticular water permeability of isolated cuticular membranes and leaf disks. *Planta* **214**: 274–282.

Slot M, Cala D, Aranda J, Virgo A, Michaletz ST, Winter K. 2021a. Leaf heat tolerance of 147 tropical forest species varies with elevation and leaf functional traits, but not with phylogeny. *Plant, Cell & Environment* **44**: 2414–2427.

Slot M, Garcia MN, Winter K. 2016. Temperature response of CO2 exchange in three tropical tree species. *Functional Plant Biology* **43**: 468–478.

Slot M, Nardwattanawong T, Hernández GG, Bueno A, Riederer M, Winter K. **2021b**. Large differences in leaf cuticle conductance and its temperature response among 24 tropical tree species from across a rainfall gradient. *New Phytologist* **232**: 1618–1631.

Slot M, Rey-Sánchez C, Winter K, Kitajima K. **2014**. Trait-based scaling of temperature-dependent foliar respiration in a species-rich tropical forest canopy. *Functional Ecology* **28**: 1074–1086.

Slot M, Rifai SW, Eze CE, Winter K. **2024**. The stomatal response to vapor pressure deficit drives the apparent temperature response of photosynthesis in tropical forests. *New Phytologist* **244**: 1238–1249.

Tredenick EC, Farquhar GD. **2021**. Dynamics of moisture diffusion and adsorption in plant cuticles including the role of cellulose. *Nature Communications* **12**: 5042.

Urban J, Ingwers MW, McGuire MA, Teskey RO. **2017**. Increase in leaf temperature opens stomata and decouples net photosynthesis from stomatal conductance in Pinus taeda and Populus deltoides x nigra. *Journal of Experimental Botany* **68**: 1757–1767.

Verryckt LT, Van Langenhove L, Ciais P, Courtois EA, Vicca S, Peñuelas J, Stahl C, Coste S, Ellsworth DS, Posada JM, *et al.* 2020. Coping with branch excision when measuring leaf net photosynthetic rates in a lowland tropical forest. *Biotropica* **52**: 608–615.

Way DA, Oren R, Kroner Y. **2015**. The space-time continuum: the effects of elevated CO2 and temperature on trees and the importance of scaling. *Plant, Cell & Environment* **38**: 991–1007.

Wolz KJ, Wertin TM, Abordo M, Wang D, Leakey ADB. **2017**. Diversity in stomatal function is integral to modelling plant carbon and water fluxes. *Nature Ecology & Evolution* **1**: 1292–1298.

Wright SJ, Kitajima K, Kraft NJB, Reich PB, Wright IJ, Bunker DE, Condit R, Dalling JW, Davies SJ, Díaz S, *et al.* 2010. Functional traits and the growth–mortality trade-off in tropical trees. *Ecology* **91**: 3664–3674.

Wu J, Serbin SP, Ely KS, Wolfe BT, Dickman LT, Grossiord C, Michaletz ST, Collins AD, Detto M, McDowell NG, *et al.* 2020. The response of stomatal conductance to seasonal drought in tropical forests. *Global Change Biology* **26**: 823–839.

Xue W, He X, Wang Q, Shi P, Lv G, Huang J, Yang D, Zhang J. **2024**. An improved representative of stomatal models for predicting diurnal stomatal conductance at low irradiance and vapor pressure deficit in tropical rainforest trees. *Agricultural and Forest Meteorology* **354**: 110098.

Yin X, Struik PC. **2009**. C3 and C4 photosynthesis models: An overview from the perspective of crop modelling. *NJAS - Wageningen Journal of Life Sciences* **57**: 27–38.

Yuan W, Zheng Y, Piao S, Ciais P, Lombardozzi D, Wang Y, Ryu Y, Chen G, Dong W, Hu Z, *et al.* 2019. Increased atmospheric vapor pressure deficit reduces global vegetation growth. *Science Advances* **5**: eaax1396.

Zhou S, Duursma RA, Medlyn BE, Kelly JWG, Prentice IC. **2013**. How should we model plant responses to drought? An analysis of stomatal and non-stomatal responses to water stress. *Agricultural and Forest Meteorology* **182–183**: 204–214.

List of Tables and Figures

Table 1. Description of the species of the study.

Species name	WD	LMA	Narea	Leaf area	T50	Foliage	PFT	N trees
Calycophyllum candidissimum DC.	0.77	69.7	1.19	14.5	50.7	Evergreen	1	3
Chrysophyllum cainito L.	0.78	109.8	1.98	67.5	49.8	Evergreen	3	2
Cinnamomum triplinerve (Ruiz & Pav.) *Kosterm.*	0.53	139.7	2.52	31.4	50.3	Evergreen	2	1
Didymopanax morototoni (Aubl.) Decne. & Planch	0.40	73.98	1.86	3381.7 (338)	50.3	Evergreen	1	1
Luehea seemannii Triana & Planch	0.59	98.7	2.02	72.7	50.1	Deciduous facultative	1	2

The wood densities (WD, in g cm^{-3}) were obtained from Wright *et al.* (2010), the leaf mass per area (LMA, in g m^{-2}) and nitrogen content (g m^{-2}) were measured in this study. The leaf area and leaflet area for compound leaves (added in parentheses, cm^2) were obtained from Slot *et al.* (2014), and the temperature at which the photosystem II functionality is reduced by 50% (T50, in °C) was obtained from Slot *et al.* (2021a). Species not included in these articles were measured following the same protocols. We classified the tree plant functional type (PFT) along the slow-fast growth continuum (1 = fast growing, 2 = intermediate, 3 = slow growing, Joseph Wright pers. communication). N trees is the number of trees for each species that could be sampled from the crane.

Table 2. Leaf conductance models used in this study to evaluate how the leaf conductance (g_{sw}) responds to changes in leaf temperature and leaf surface relative humidity.

Model	f(A)	f(VPD_{leaf})	g_{sw}	X	$g_{sw,dark}$
1	A_n	$\frac{1}{\sqrt{VPD_{leaf}}}$	$g_0+1.6g_1\frac{A_n}{\sqrt{VPD_{leaf}}C$	$1.6\frac{A_n}{\sqrt{VPD_{leaf}}C$	$g_0-1.6g_1\frac{R_{dark}}{\sqrt{VPD_{leaf}}C$
2	A_n	RH	$g_0+1.6g_1\frac{A_nRH}{CO_2}$	$1.6\frac{A_nRH}{CO_2}$	$g_0-1.6g_1\frac{R_{dark}RH}{CO_2}$
3	A_g	$\frac{1}{\sqrt{VPD_{leaf}}}$	$g_0+1.6g_1\frac{A_g}{\sqrt{VPD_{leaf}}C$	$1.6\frac{A_g}{\sqrt{VPD_{leaf}}C$	g_0
4	A_g	RH	$g_0+1.6g_1\frac{A_gRH}{CO_2}$	$1.6\frac{A_gRH}{CO_2}$	g_0
5	A_g^2	$\frac{1}{\sqrt{VPD_{leaf}}}$	$g_0+1.6g_1\frac{A_g^2}{\sqrt{VPD_{leaf}}C$	$1.6\frac{A_g^2}{\sqrt{VPD_{leaf}}C$	g_0
6	A_g^2	RH	$g_0+1.6g_1\frac{A_g^2RH}{CO_2}$	$1.6\frac{A_g^2RH}{CO_2}$	g_0

We compared different functions to represent the effect of the photosynthesis rate A on $g$sw ($f(A)$) and the effect of the evaporative demand $f(VPD)$. A_n represents the net photosynthesis rate, and A_g the gross photosynthesis rate. RH represents the air relative humidity in percent, VPD_{leaf} represents the air to leaf vapor pressure deficit in kPa, and CO_2 represents the CO_2 concentration at the leaf surface (ppm). On the right-hand side of the g_{sw} equations, a change in RH impacts VPD_{leaf} and a change in T_{leaf} impacts A_n and A_g as well as VPD_{leaf}. All these models are linear models ($g_{sw} = g_0 + g_1X$) where g_0 and g_1 are the intercept and slope, respectively, and X is a composite variable representing the regressor.

Table 3. Temperature dependence parameters of the dark respiration (R_{dark}) using a Peak function (Equation 4).

Species	R_{dark25}	E_a	H_d	AIC Arrhenius	AIC Peak
C. candidissimum	0.75 ± 0.10	59.6 ± 5.3	158.9 ± 1.3	-10.3	-13.5
C. cainito	0.69 ± 0.07	67.3 ± 6.4	156.8 ± 1.1	-21.8	-28.1
C. triplinerve	0.69 ± 0.04	61.0 ± 5.2	156.7 ± 0.7	-22.3	-40.2
D. morototoni	0.50 ± 0.06	85.9 ± 9.0	156.2 ± 1.0	9.3	-8.3
L. seemannii	1.13 ± 0.05	56.7 ± 2.8	159.1 ± 0.7	-19.9	-32.7

R_{dark25} is the dark-adapted leaf respiration at 25 °C in μmol m^{-2} s^{-1}, E_a and H_d are the energy of activation and the enthalpy of deactivation of the reaction in kJ mol^{-1}, respectively, and AIC Arrhenius and AIC Peak represents the Akaike Information Criterion for the Arrhenius equation (Equation 3) and the Peak function (Equation 4), respectively. Since the Peak function always better represented the R_{dark} temperature dependence (lowest AIC Peak), we only show the parameters for this equation.

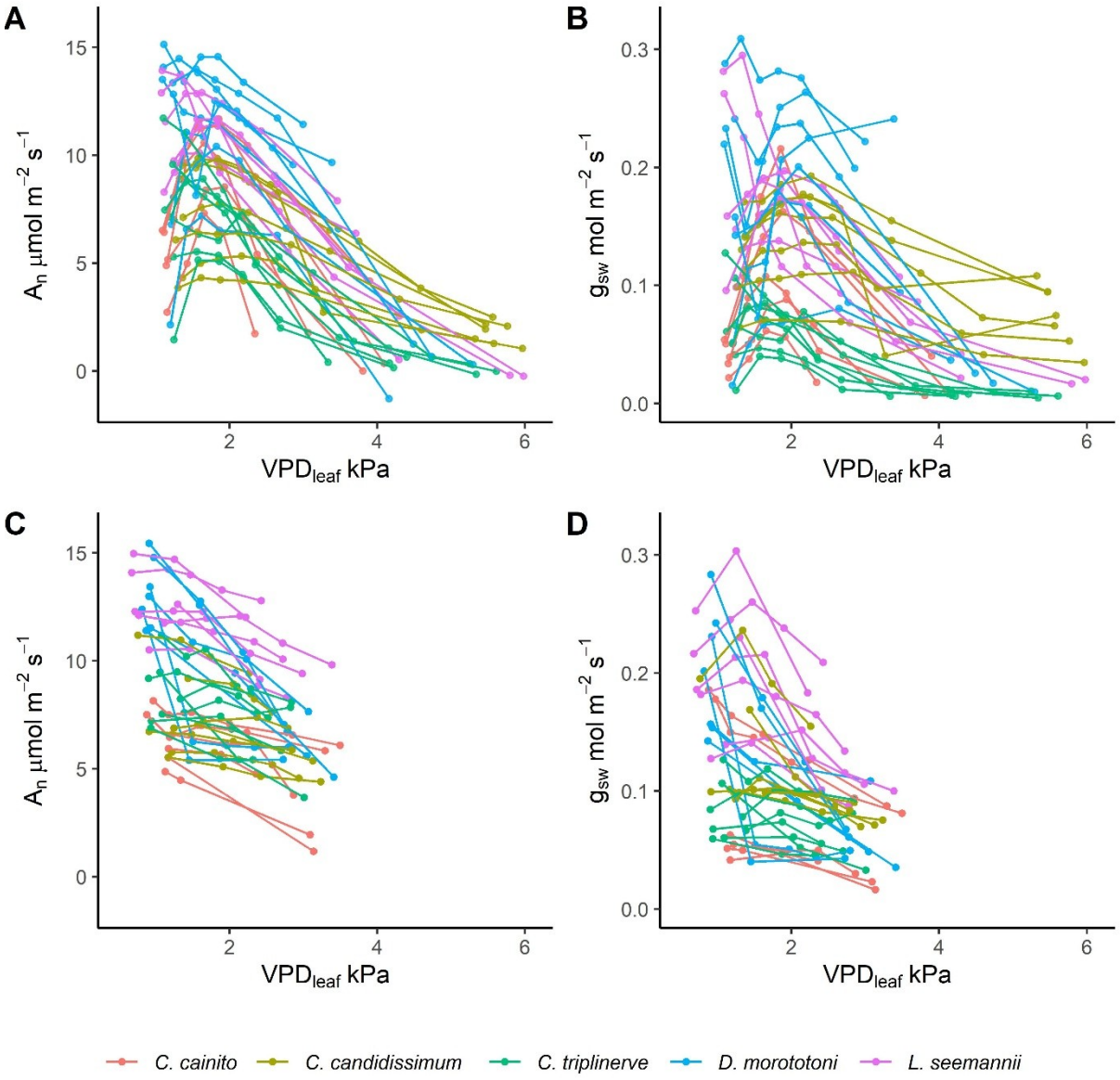

Figure 1. Photosynthesis (A_n) and conductance (g_{sw}) response of five tropical species to changes in leaf-to-air water vapor pressure difference (VPD_{leaf}). VPD_{leaf} was modified by increasing the leaf temperature at constant relative humidity (constant at 55 to 60 % during each curve, A and B) or by decreasing the relative humidity at constant leaf temperature (constant at 25 to 30 °C during each curve, C and D). In all the panels, the points represent one measurement made on one leaf, the lines represent each leaf, and the color represents the five different species that we measured.

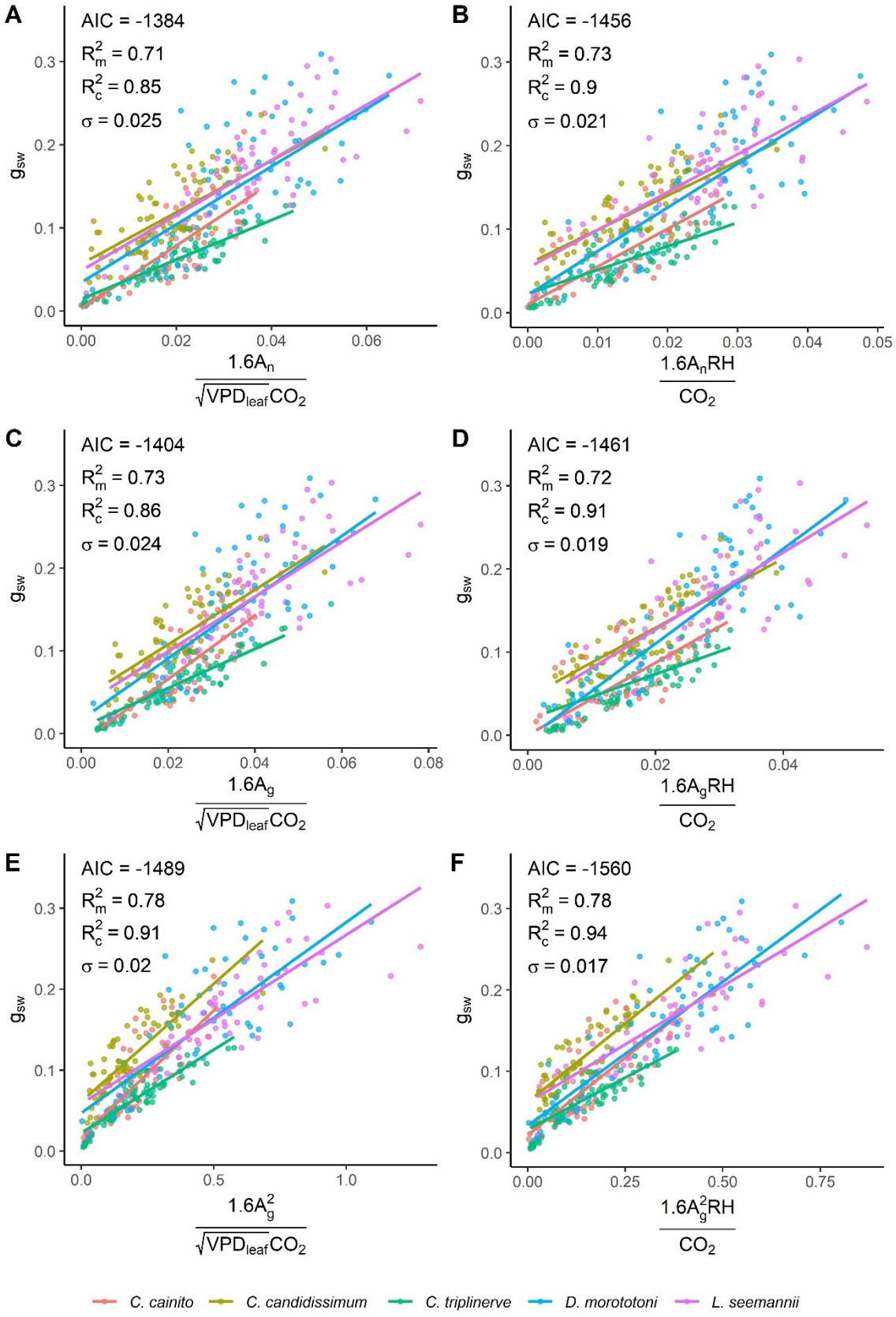

Figure 2. Relationships between leaf conductance (g_{sw}) and the regressor of six stomatal models differing in their representation of the evaporative demand and photosynthesis. The evaporative

demand is represented on the left panels by leaf-to-air water vapor pressure difference (VPD_{leaf}), and on the right panels by the relative humidity (RH). Photosynthesis is modeled by: (A,B) net photosynthetic rate (A_n); (C,D) gross photosynthetic rate (A_g); (E,F) squared gross photosynthetic rate (A_g^2). Each point corresponds to a gas exchange measurement, and each color a tropical tree species. Each line corresponds to the mean effect of the species estimated by a linear regression between g_{sw} and the regressor with a leaf random effect on the relationship. The leaf conductance was varied by modifying the relative humidity and leaf temperature under constant CO_2 and light conditions. AIC is the Akaike Information Criterion, R_m^2 and R_c^2 are the conditional and marginal coefficient of determination of the mixed model, respectively, and σ is the standard deviation of the residuals.

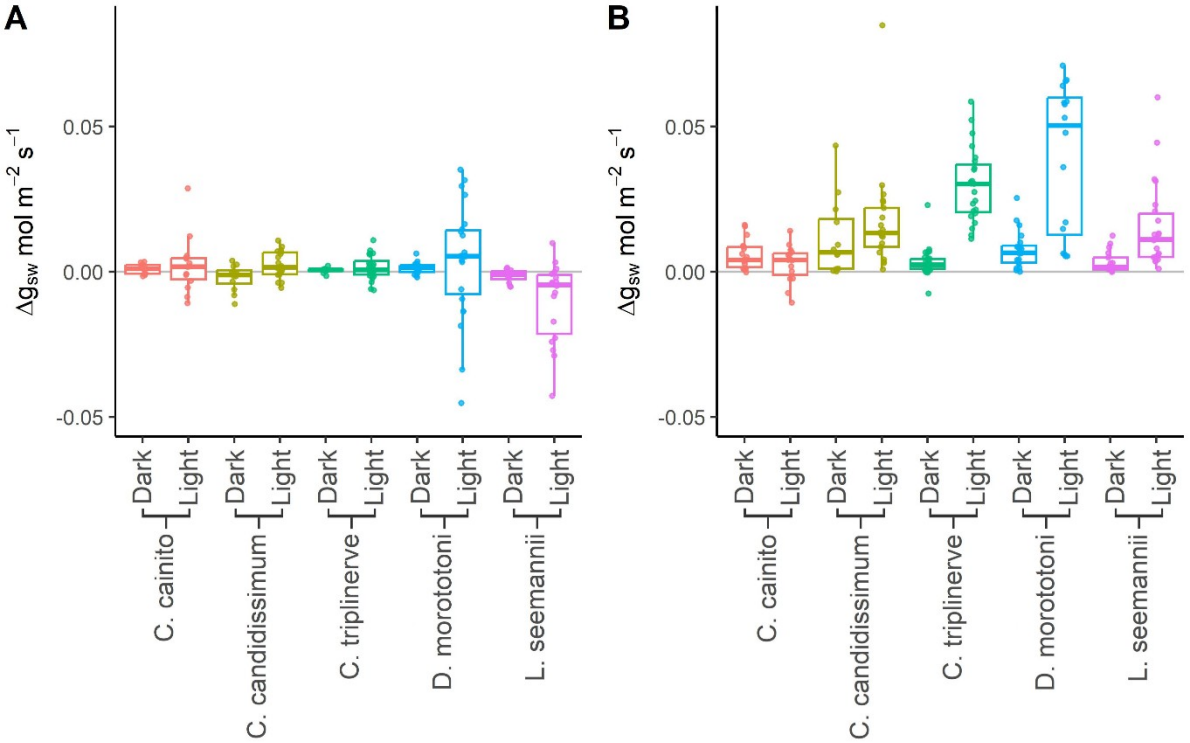

Figure 3. Quick change in conductance (Δg_{sw}) two minutes after an increase in leaf temperature (panel A) or a decrease in relative humidity (panel B) for the five species (x axis), in the dark and in the light (400 µmol m^{-2} s^{-1}). A Δg_{sw} above zero corresponds to a wrong-way response as an increase in the vapor pressure difference when the temperature increases or the humidity decreases is expected to decrease g_{sw}.

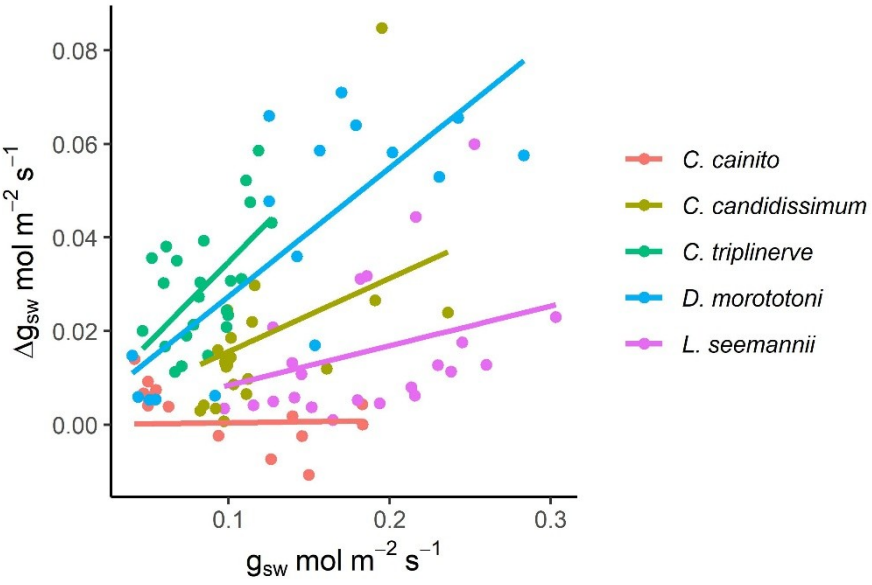

Figure 4. Effect of the leaf conductance (g_{sw}) on the intensity of the wrong-way response (Δg_{sw}) produced by a change in relative humidity. Each line corresponds to the mean effect of the species estimated by a linear regression between Δg_{sw} and g_{sw} with a fixed zero intercept and a leaf random effect on the relationship. The slope of the regression was significantly different from zero for all the species except for *C. cainito*.

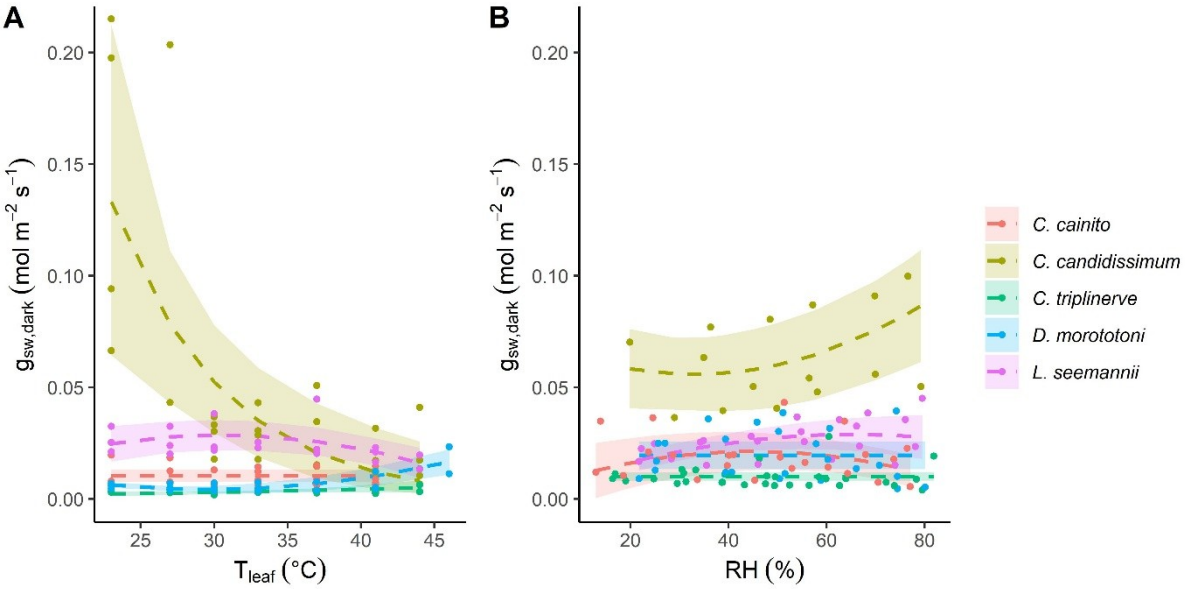

Figure 5. Dark-adapted leaf conductance ($g_{sw,dark}$) response to leaf temperature (T_{leaf}, A) and relative humidity (*RH*, B). Each point represents a measurement, and the lines represent the species mean $g_{sw,dark}$ response as modeled by the best model fit of linear, quadratic and exponential regressions (Table S5). The shaded areas represent the confidence interval of the mean. The $g_{sw,dark}$ response to T_{leaf} was conducted at an average *RH* of 52.8 ± 1.9 % and the $g_{sw,dark}$ response to *RH* was conducted at a constant T_{leaf} of 26.6 ± 1.1 °C.

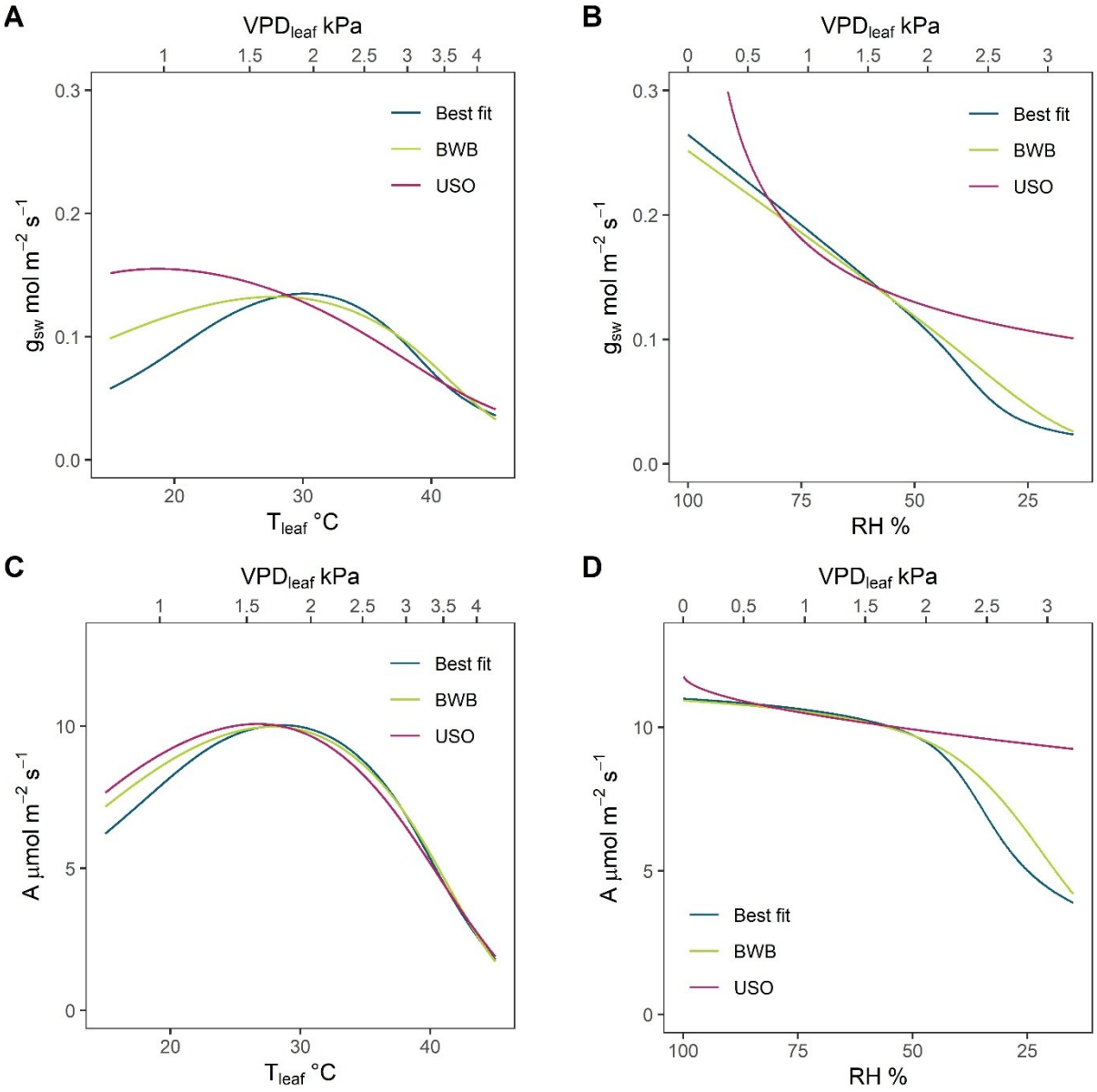

Figure 6. Simulation of leaf conductance (g_{sw}) and photosynthesis (A_n) response to leaf temperature (T_{leaf}) and air relative humidity (*RH*) made by coupling the g_{sw} models with the Farquhar *et al.* (1980) photosynthesis model. Three g_{sw} models are compared: USO (Medlyn *et al.,* 2011, Equation 1), BWB (Ball *et al.*, 1987, Equation 2), and the best fit model from this study. For the three g_{sw} models, the parameters g_0 and g_1 were set to the average value measured in this study. The parameters used for the Farquhar *et al.* (1980) model were V_{cmax25}, J_{max25}, and R_{dark25} measured on the same species (46, 83, and 0.75 µmol m^{-2} s^{-1}, respectively). The temperature dependence of V_{cmax25} and J_{max25} was modeled using Kumarathunge *et al.* (2019) equations for plant growing at 26°C, and the R_{dark25} temperature dependence was modeled using the average parameters from this study (Table 3). The input variables CO_2 and irradiance were set constant at 400 ppm, and 400 µmol m^{-2} s^{-1}, respectively. *RH* was set to 55% in panels A and

C, and T_{leaf} was set to 28°C in panels B and D. In both panels, a second X axis with the leaf-to-air vapor pressure difference (VPD_{leaf}) was added at the top of the plot.